

Articles

Tripod-like Cationic Lipids as Novel Gene Carriers

Asier Unciti-Broceta,[†] Emma Holder,^{‡,§} Lisa J. Jones,^{‡,§} Barbara Stevenson,^{‡,§} Andrew R. Turner,[†] David J. Porteous,^{‡,§} A. Chris Boyd,^{‡,§} and Mark Bradley^{*,†}

School of Chemistry, West Mains Road, University of Edinburgh, Edinburgh EH9 3JJ, U.K., Medical Genetics, Molecular Medicine Centre, University of Edinburgh, Edinburgh EH4 2XU, U.K., and the U.K. Cystic Fibrosis Gene Therapy Consortium

Received September 18, 2007

An innovative family of tridentate–cationic “single-chained lipids” designed to enhance DNA compaction and to promote endosomal escape was synthesized by coupling various lipids to a multibranched scaffold. DNA retardation assays confirmed the ability of the most members of the library to complex DNA. Classical molecular dynamics simulations performed on the lauryl derivative, bound to a short strand of DNA in aqueous solution supported these observations. These showed that two “arms” of the tripodal molecule are ideally suited to forming strong Coulombic interactions with two contiguous phosphate groups from the DNA backbone while the lipophilic tail stays perpendicular to the DNA helix. Gene transfer abilities of the library were assessed in multiple cell lines (CHO, Cos7, and 16HBE14o-) with some library members giving excellent transfection abilities and low cytotoxicity, supporting the use of this tripodal approach for the development of efficient gene delivery agents.

Introduction

Viral gene delivery, as a molecular biology tool or as a potential therapeutic approach, is without doubt the most efficient method of DNA delivery (transfection) to date. However, because of the disadvantages of viral vectors (antigenicity, production cost, limited size of cargo, etc.),^{1,2} nonviral delivery systems represent a very attractive alternative, especially because of their relatively low cost and procedural simplicity. Despite numerous improvements, the *in vivo* efficacy of nonviral vectors still needs to be increased for both clinical and research purposes.³

Among the nonviral vectors, cationic lipids are perhaps the only class of compounds in which rational design can be readily applied and structure–activity relationships studied.⁴ Generally speaking, cationic lipids are composed of a lipophilic component attached through a linking motif to a positively charged, polar headgroup.^{4,5} When these compounds are mixed with DNA or RNA in an aqueous solution, electrostatic and hydrophobic interactions lead to self-assembly and self-organization into a liposome-like complex known as a lipoplex,⁶ although the exact nature of these complexes is still subject to debate. These formulations are often supplemented by the addition of a neutral surfactant, such as DOPE,^a which usually improves the transfection abilities of the mixture.⁷ Because of its fusogenic

properties,^{7–9} this so-called “co-lipid” seems to promote endosomal escape of DNA once the cell has encapsulated the lipoplex by endocytosis, a step that may well be the most critical in the entire transfection process.

A very wide range of cationic lipids have been synthesized to date,⁴ and several are commercially available.^{10–13} Typically, the cationic headgroups found in these families of synthetic materials are nitrogen-based motifs and the lipid moiety is composed of two long chain fatty acids or a cholesterol derivative. Although single-chained agents are expected to complex DNA^{4,14,15} by forming micelles,¹⁶ such vectors are traditionally considered to be more toxic and less efficient than their double-tailed counterparts.¹⁷ However, this generalization is not always correct.^{18,19} Indeed, the use of single-chained cationic vectors could offer an accelerated means of allowing endosomal disruption and thus enhance DNA escape. This hypothesis formed the basis of the work reported here.

Results and Discussion

Design and Computational Modeling. Because of the importance of achieving optimal DNA condensation,²⁰ the nature of the polar headgroups was addressed in a manner to enhance the packing properties of an amphiphilic, single-chained lipid transfection agent. A multivalent cationic lipid was therefore devised consisting of three primary amines connected through an alkyl linker to a central carbon core, which was linked via an amide bond to the hydrophobic tail. This novel polyamine lipid was expected to adopt a tripod-like conformation, enhancing its interaction with nucleic acids.

A set of both quantum mechanical and classical calculations were performed to study the 3D structure of this chemical model in a number of different environments (see Supporting Information for details of these calculations). Quantum mechanics in the form of density functional theory (DFT) calculations were used to elucidate the gas phase structure of the cationic lipid, and according to its optimized geometry (see Figure 1), the lipid

* To whom correspondence should be addressed. Phone: 0044-131-6504820. Fax: 0044-131-6506453. E-mail: Mark.Bradley@ed.ac.uk.

[†] School of Chemistry, University of Edinburgh.

[‡] Molecular Medicine Centre, University of Edinburgh.

[§] U.K. Cystic Fibrosis Gene Therapy Consortium.

^a Abbreviations: DOPE, dioleyl phosphatidyl ethanolamine; DCC, di-cyclohexylcarbodiimide; DMAP, 4-dimethylaminopyridine; TFA, trifluoroacetic acid; CF, cystic fibrosis; DOTAP, *N*-[1-(2,3-dioleyloxy)propyl]-*N,N,N,N*-trimethylammonium methylsulfate; PEI, poly(ethyleneimine); DFT, density functional theory; MD, molecular dynamics; RLU/mg, relative luminescence units per milligram of protein. Fatty acid tails are described using a “*C_n:m*” format, with “*n*” defining the number of carbon atoms and “*m*” the number of unsaturated bonds.

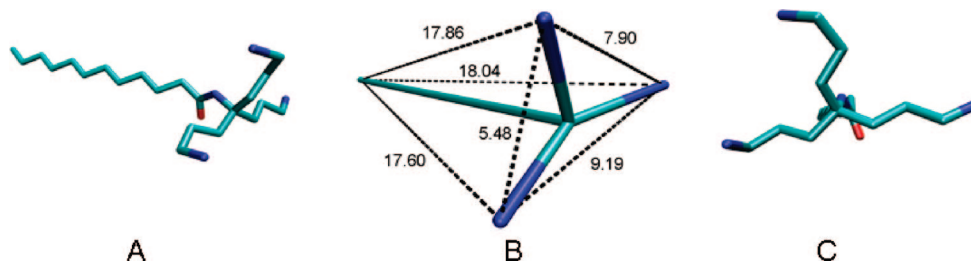


Figure 1. DFT optimized gas-phase structure. The molecular modeling corresponds to the chloride salt of the lauryl (C12:0) derivative. Hydrogen atoms and chloride ions are not shown, and distances are in angstroms. (A) and (C) are different perspectives of the structure. (B) is a tripodal construction created by connecting with lines the five reference atoms of the molecule: the three nitrogen atoms of the ammonium groups (in dark blue), the central quaternary carbon, and the last carbon of the lipid tail.

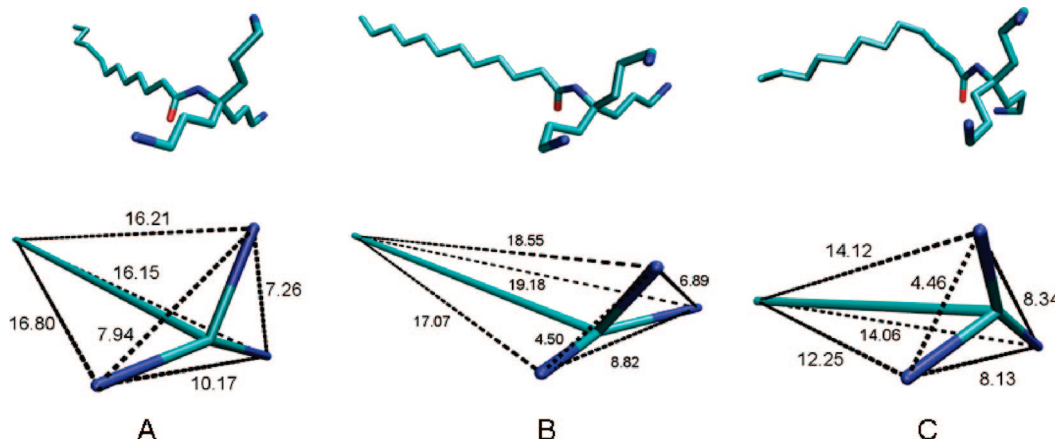


Figure 2. Chemical conformation of the amphiphilic compound in different environments: (A) in water; (B) in the gas phase; (C) in chloroform. The top line shows a snapshot of the molecular structures (without hydrogen atoms and chloride anions) and the bottom line illustrates the structure of the tripods (all distances in angstroms). (A) and (C) correspond to snapshots from MD trajectories, while (B) corresponds to the optimized gas-phase structure using the classical model.

adopts a tripod-like structure, as expected, with the tripodal ammonium plane nearly perpendicular to the hydrophobic tail.

To understand the structure of the lipid in different solvation environments classical molecular dynamics (MD) simulations were performed on the lipid in water (polar solvent) and chloroform (nonpolar solvent). The adaptation of the structure's conformation to these different environments can clearly be observed from Figure 2. In aqueous solution the lipid forms a true tripodal structure with the nitrogen plane perpendicular to the hydrocarbon tail and the three "arms" of the tripod evenly extended into the solvent. Over the course of the simulations, the chloride ions diffuse away from the lipid and become fully solvated. In the nonpolar solvent the tripod becomes distorted as the cationic lipid salt attempts to minimize the interactions between its ionic moieties and the solvent. Two nitrogen "arms" come into proximity (4.46 Å) and share close interactions with two of the chloride ions. The remaining nitrogen "arm" folds back toward the carboxyl group on the tail, taking the remaining chloride ion with it. No diffusion of the chloride ions into the solvent is observed during the simulations. These elements combine to distort the tripod such that the "arms" no longer extend into the solvent and the nitrogen plane is no longer perpendicular to the hydrocarbon tail. Although the images in Figure 2 are just snapshots from the MD trajectories, analysis of the radial distribution functions reveal the same trends throughout the whole simulation (see Supporting Information).

To investigate the nature of the tripodal lipid binding to DNA, classical MD simulations were performed on a single lipid molecule bound to a short α helix of double stranded DNA (16 A-T base pairs) in aqueous solution. A snapshot from the simulations of the lipid bound to DNA is shown in Figure 3.

Radial distribution functions in the Supporting Information illustrate that the lipid molecule maintains a tripodal form throughout the entire simulation.

The calculations illustrate that two "arms" of the amphiphilic molecule are ideally suited to forming strong Coulombic interactions with two contiguous phosphate groups from the DNA backbone while the third protonated amine remains solvated by molecules of water (see Figure 3 for a snapshot of the simulation or the complete movie in the Supporting Information). During the simulation, the lipophilic tail is extended perpendicularly to the DNA helix (see Figure 3A,B). As the simulation progresses, the cationic lipid diffuses into the solvent, indicating that the electrostatic interactions are not sufficient to maintain a stable complex with the DNA, highlighting the importance of additional hydrophobic interactions in assisting the formation of a stable layer of amphiphilic molecules around the DNA.

These exploratory calculations suggest that the electrostatic interactions between the tripodal surfactant and the DNA may lead to organization of the lipids around the sugar-phosphate backbone and simultaneously promote hydrophobic interactions among the regularly disposed fatty tails, assisting lipoplex formation and modulating its stability and structural evolution. As a consequence of the proposed binding scheme, this kind of tripod-like amphiphilic chemicals is expected to complex DNA at low charge ratios.

Synthesis. The library was synthesized by coupling different lipid derivatives to the common intermediate tris[3-(*N*-*t*er-butoxycarbonylaminoo)propyl]methylamine **4**. The preparation of **4** was accomplished as previously reported²¹ from trinitrile **1** (see Scheme 1). Briefly, hydroboration of compound **1** gave

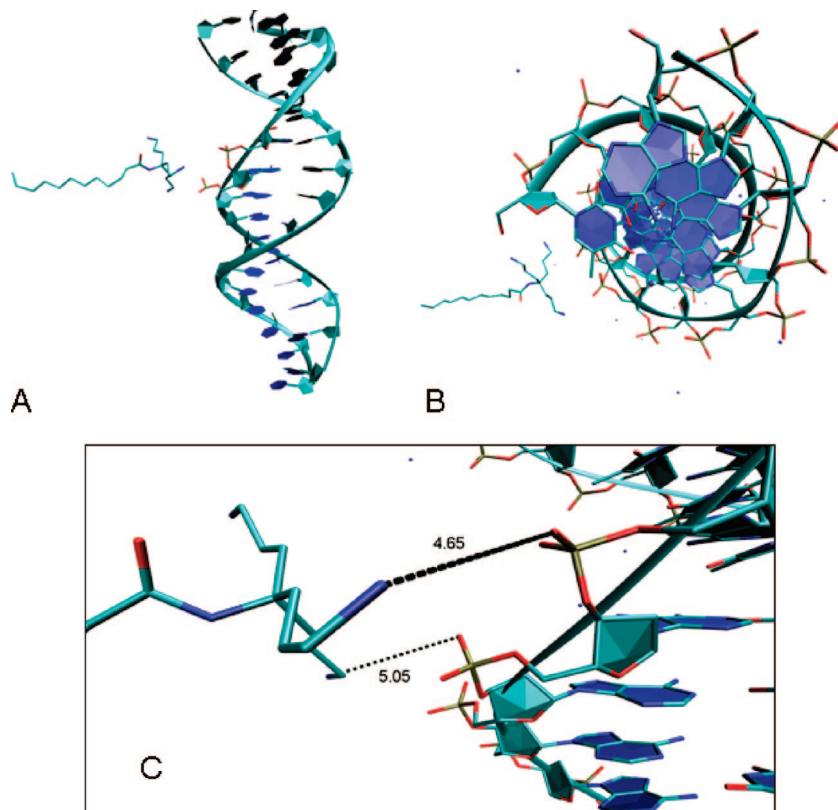


Figure 3. Snapshot from MD simulation of the cationic lipid bound to DNA (solvent, hydrogens, and counterions are not shown): (A) lateral view; (B) view from above; (C) zoomed-in view of the lipid–DNA interaction with the N...O distances illustrated (in angstroms).

triamine **2** which was, after workup (but no further purification), treated with di-*tert*-butyl dicarbonate (Boc₂O) and Et₃N in refluxing methanol and subsequently purified to give tricarbamate **3** in good yield (72%, two steps). Catalytic hydrogenation of the nitro derivative **3** with Raney nickel gave amine **4** in high yield (90%).

The tunable component in the structure of this new family of cationic lipids is the length of the hydrophobic chain. This parameter, along with the polar headgroups, influences the supramolecular association that generates the lipoplex and seems to be particularly important in the release mechanism of the plasmid from the early endosome.⁴ Consequently amine **4** was coupled with 16 different lipid moieties in order to evaluate the influence of the chain length and the presence of unsaturation on the biological properties of these new vectors. Coupling was achieved as shown in Scheme 1 with either DCC or acyl chloride mediated coupling to give **5a–p**. Removal of the *N*-Boc protecting group and subsequent salt formation was performed under acidic conditions (with 4 N HCl in dioxane or 1:1 dioxane/water). The HCl salt was preferred over other forms (such as the TFA salt) for toxicity reasons.²²

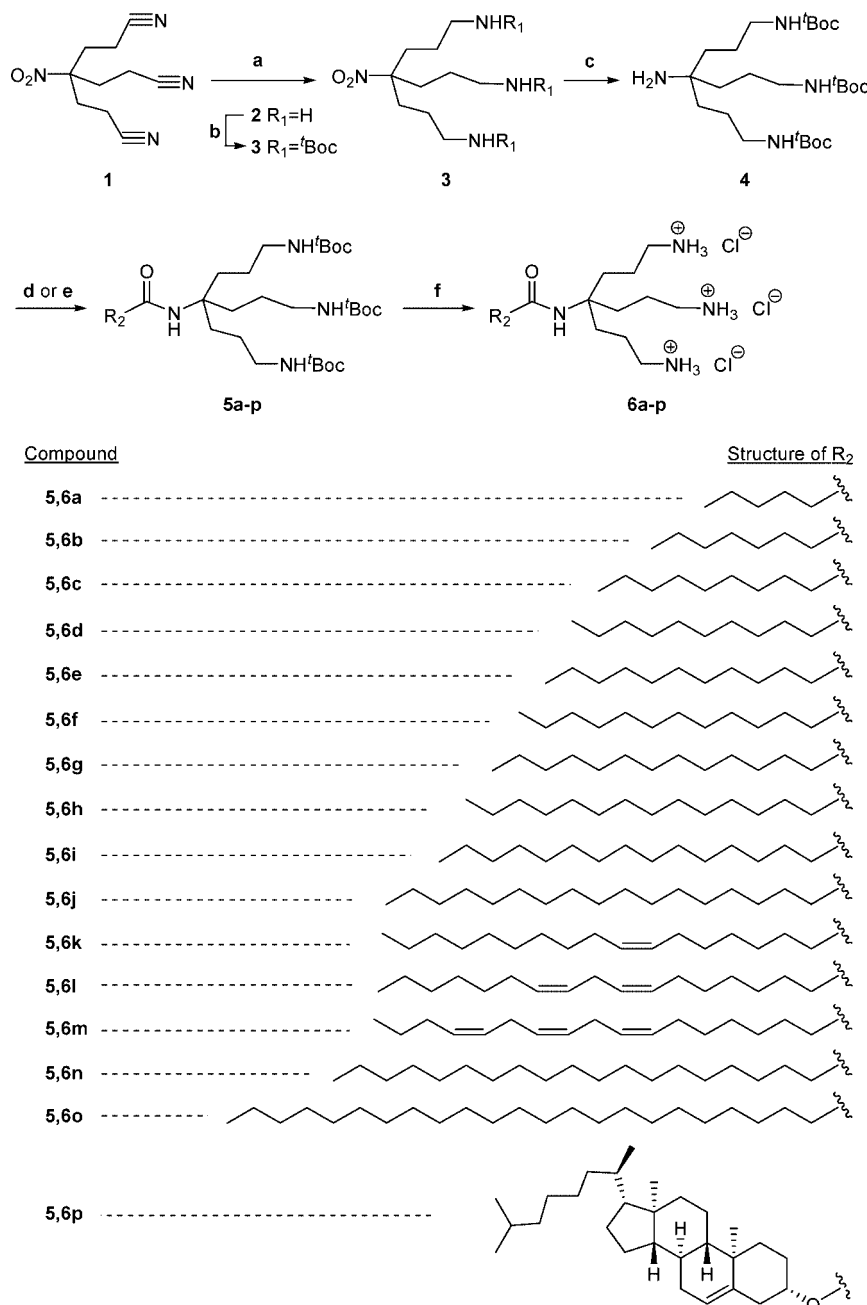
DNA Retardation Assays. The electrostatic binding interactions between DNA and compounds **6a–p** were studied by conventional electrophoretic DNA retardation assays.²³ Lipoplexes were formulated as a function of their lipid/DNA charge ratios (*N/P*) (see section 2.1 of the experimental section for a description of these terms). Representative electrophoretic gel patterns are shown in Figure 4. As expected, experiments showed that the longer the fatty tail, the greater the ability to retard DNA. Lipids **6a–c** were not able to retard plasmid mobility at any of the *N/P* ratios tested, while lipids **6d–g** showed a capacity to retard DNA which was strongly influenced by the charge ratio. Compounds **6h** (C15:0) to **6p** (cholesteryl)

completely inhibited the electrophoretic mobility of plasmid DNA, even at a charge ratio of 1.5, meaning that DNA immobilization required less than a molecule of lipid per pair of nucleotides. These experimental results agree with the efficient electrostatic interactions observed between the lipid and the DNA in the MD simulations (Figure 3).

Interestingly, ethidium bromide was much less efficient at staining the plasmid when complexed with **6h–p**, evidence of the efficacy with which these compounds complex DNA, preventing ethidium bromide entry into the lipoplex. Treatment of the preformed DNA/ethidium bromide complex with the cationic lipids also resulted in a chain length dependence release of ethidium bromide, with the longer chain lipids being more efficient (see Figure 5).

Gene Transfer Studies. Preliminary assays (see section 3 in Supporting Information) supported the use of DOPE (as a co-lipid) and serum-free media for enhancing the transfection properties of the family of compounds, and thus, all subsequent assays were realized under these conditions.

The gene transfer efficiency of the library was evaluated in two ubiquitous cell lines, Chinese hamster ovary (CHO) and African green monkey kidney (Cos7), employing pLux²⁴ as luciferase-reporter vector. Lipoplexes were formulated at a variety of *N/P* ratios (1.5, 3, and 6) using DOPE (1:1 molar ratio) as a helper lipid (see section 2.3 for full experimental protocols). Cells transfected with Lipofectamine2000/pLux complexes and untreated cells were used as positive and negative controls respectively. As expected, analysis of the luciferase activity showed that the transfection ability of the compounds was strongly dependent on the length and type of the hydrophobic moiety (see Figure 6). Significant gene expression (*p* < 0.05 when compared to the nontransfected control group) was detected after transfection with the majority of lipoplexes.

Scheme 1^a

^a Reagents and conditions: (a) $BH_3 \cdot THF$ (6 equiv), dioxane, 60 °C, 20 h; (b) Boc_2O (3 equiv), DCM, 73% (two steps); (c) H_2 (1 atm), Raney Ni, EtOH, 24 h, stirring at 700 rpm, 88%; (d) fatty acid, DCC, DMAP (cat.), DCM, 2 h, 85–97%; (e) acyl chloride or cholesteryl chloroformate, Pyr, DMAP (cat.), DCM, 2 h, 83–95%; (f) 4 N HCl in dioxane or in 1:1 water/dioxane, 2–4 h, quantitative yield.

Negative or low luciferase expression was only detected with lipids **6a–c**, which was in accordance with their low ability for complexing DNA (see Figure 4). In the library, fatty tails (C12–15:0 and C24:0) dissimilar to the most abundant ones found in the cell membranes (C16:0 and C18:0) appeared to have good transfection efficiency. Luciferase activity was especially high with some formulations of lipid **6e** (*N/P* 3), **6f** (*N/P* 1.5), and **6o** (*N/P* 1.5, 3 and 6). The results with lipids **6e** and **6f** (C12:0 and C13:0, respectively) are consistent with previous work²⁵ that underlined the probable role of short lipid chains in facilitating intermembrane mixing, an important factor in the endosomal escape of DNA. Interesting, however, was the potency of the lignoceryl derivative **6o** (C24:0), which showed high luciferase activity at various charge ratios (all three for CHO cells and *N/P* of 3 and 6 for Cos7) although containing

the longest lipid moiety investigated. This observation is remarkable as to date most groups have avoided going beyond C18 chain lengths and suggests that this limitation may not be entirely justified. However, there is the possibility that the transfection properties demonstrated by the very long fatty derivatives may be restricted to single-chained cationic lipids.

Because of our interest in gene therapy for cystic fibrosis (CF), we subsequently assessed the gene transfer efficiency of these novel cationic lipids in an airway epithelial cell line. CF is the most common lethal autosomal recessive genetic disease in the Caucasian population and is caused by a mutation in the cystic fibrosis transmembrane conductance regulator gene. Although several organs are affected, lung disease is the major cause of morbidity and mortality in CF patients.²⁶ Because previous studies have shown that nonviral gene transfer agents

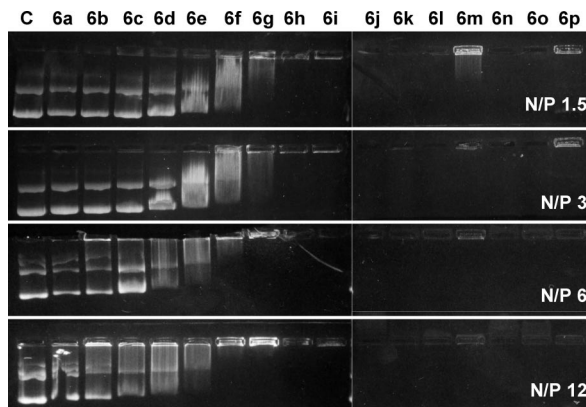


Figure 4. Gel retardation assay. Compounds **6a–p** were complexed with pLux at various charge ratios, loaded in an agarose gel (1% agarose, 1 μ g/mL ethidium bromide in TBF buffer), and run at 100 V for 30 min. C = naked pLux.

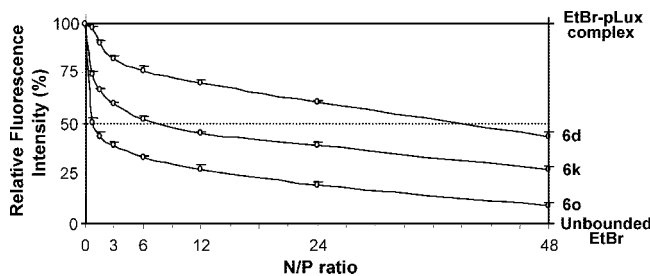


Figure 5. Relative fluorescence intensity as a function of the quantity of cationic lipid added. Compounds **6d**, **6k**, and **6o** were added to a preformed EtBr–pLux complex (molar ratio = 1) at different charge ratios (0.75, 1.5, 3, 6, 12, 24, and 48) and then analyzed with a spectrofluorometer (excitation at 510 nm; emission at 600 nm). Fluorescence results are presented with 100% defined as the fluorescence intensity of the original EtBr–pLux complex and 0% defined as the fluorescence intensity of the noncomplexed ethidium bromide.

can be effectively readministered to the lung,²⁷ we tested the novel library in terms of transfection efficiency and cell toxicity on a human bronchial epithelial (16HBE14o-) cell line. Besides using Lipofectamine 2000 as a positive control, we also compared gene expression to PEI and DOTAP, which are agents routinely used to deliver DNA to the lung *in vivo*. As before, the data analysis showed significant ($p < 0.05$ when compared to the nontransfected control group) luciferase activity with most of the library members (see Figure 7), and encouragingly some of them were significantly ($p < 0.05$) better than DOTAP (formulations highlighted with arrows in Figure 7), which has previously been used in a CF clinical trial.²⁸ High transfection efficiency was again observed with a number of *N/P* ratios from lipids **6e**, **6f**, and **6o** and also with the cholesteryl derivative **6p** (*N/P* of 3 and 6). These activities were remarkably better than DOTAP and comparable to PEI.

Toxicity Studies. The MTT assays showed overall high cell viability at the concentrations of compounds tested (see section 5 of the Supporting Information).

Optimization of Cationic-Lipid/DOPE ratios. To study the influence of DOPE on the transfection abilities of the novel compounds, lipids **6o** and **6p** were screened with DOPE at a variety of molar ratios (1:0, 1:0.5, 1:1, 1:1.5, and 1:2) and tested with CHO cells (Figure 8). Analysis revealed that the presence of DOPE greatly enhanced the transfection abilities of compound **6o**, with an optimal ratio of 1:1.5 (Figure 8A). An increase in gene expression was also observed when increasing DOPE ratios

for lipid **6p**, with a molar ratio 1:2 giving the highest transfection abilities (Figure 8B).

Size Determination of Lipid **6o Aggregates as Aqueous Dispersions.** Compound **6o** was one of the most active compounds, and its formulations were therefore analyzed in more depth by dynamic light scattering in order to gain information on its aggregation properties (this was done in the transfection media and in the absence and presence of DOPE). Analysis of lipid **6o** with and without DOPE (but no DNA) generated particles of 427 ± 38 and 387 ± 98 nm respectively. Aiming to find correlation between the lipoplex size distribution and the transfection results, particle size analysis was carried out on the **6o**/pLux and **6o**/DOPE/pLux formulations as used for the optimization transfection experiments (Figure 8A). Table 1 shows the particle size distributions of the lipoplexes formed by lipid **6o** as formulated at five **6o**/DOPE molar ratios (1:0, 1:0.5, 1:1, 1:1.5, and 1:2) and complexed at three charge ratios with pLux (1.5, 3, and 6). Interestingly, the lipoplexes formulated with an *N/P* ratio of 6 (entries 11–15 of Table 1), which gave lower transfection efficacies in CHO cells, generated the smallest particles. It is important to note that the lipoplexes were found to be stable over 24 h.

Conclusions

Novel cationic lipids composed of a single fatty tail and three positive headgroups were designed with the purpose of achieving optimal condensation of DNA and enhancing transfection. Computational studies showed that two “arms” of the amphiphilic molecule are ideally suited to forming strong Coulombic interactions with two contiguous phosphate groups from the DNA backbone while the lipophilic tail stays perpendicular to the DNA helix, maybe assisting lipoplex formation. A 16-member library of tripod-like cationic lipids was prepared by varying the hydrophobic moiety of the structure and evaluated on the basis of the influence of the chain length and the presence of unsaturation. DNA retardation assays verified the high capacity of the longer-chain derivatives to complex DNA even at low charge ratios. The gene transfer efficiency demonstrated in CHO, Cos7, and 16HBE14o- cell lines along with the low cytotoxicity of the compounds underline the promising features of this innovative tripod-like structure, supporting the application of some members of the library for *in vivo* purposes. Finally, the transfection data obtained from the lignoceryl derivative (**6o**) also suggest that tail lengths of 20 carbon atoms or more for cationic lipid libraries would be worthy of further investigation.

Experimental Part

1. Synthesis and Characterization of the Novel Compounds.
1.1. General Information. All commercially available chemicals were reagent grade and were used without further purification. Unless otherwise indicated, all the reactions were performed at room temperature. Flash chromatography employed Merck silica gel (Kieselgel 60 (0.040–0.063 mm)), and analytical TLC was performed with 0.2 mm silica-coated aluminum sheets, with visualization by dipping in a solution of ninhydrin (0.3% in weight in *n*-butanol containing 3% acetic acid in volume). Eluents used were analytical grade. NMR spectra were recorded using a Bruker ARX250 spectrometer operating at 250 MHz for ¹H and 62.5 MHz for ¹³C and DEPT at 298 K. Chemical shifts are reported in ppm and were referenced to residual solvents resonances. All coupling constants (*J* values) were measured in Hz. DEPT interpretations appear in parentheses. Low resolution mass spectra (LRMS) were recorded using a VG Platform quadrupole electrospray ionization (ES+) mass spectrometer. Salts **6a–p** mass spectra were also acquired by high-resolution fast-atom bombardment (FAB+) mass spectrometry.

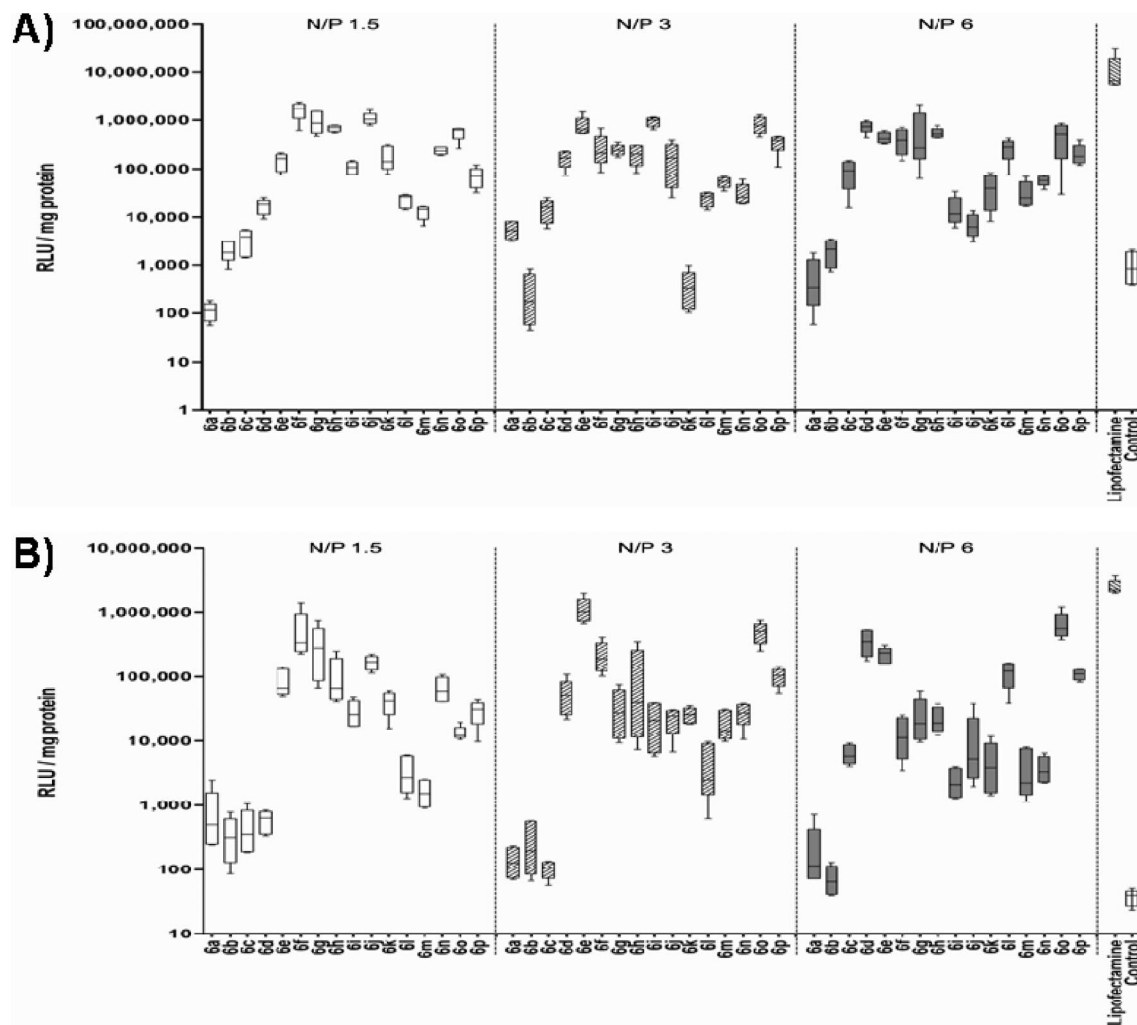


Figure 6. Luciferase activity, expressed as relative light units per milligram of protein (RLU/mg protein), of compounds **6a–p** complexed with pLux at various charge ratios in CHO (A) and Cos7 (B) cell lines. Data are shown as a box and whisker plot. The box extends from the 25th to the 75th percentile, the line indicates the median, and the whiskers extend from the highest to the lowest value. $n = 6$ wells/group.

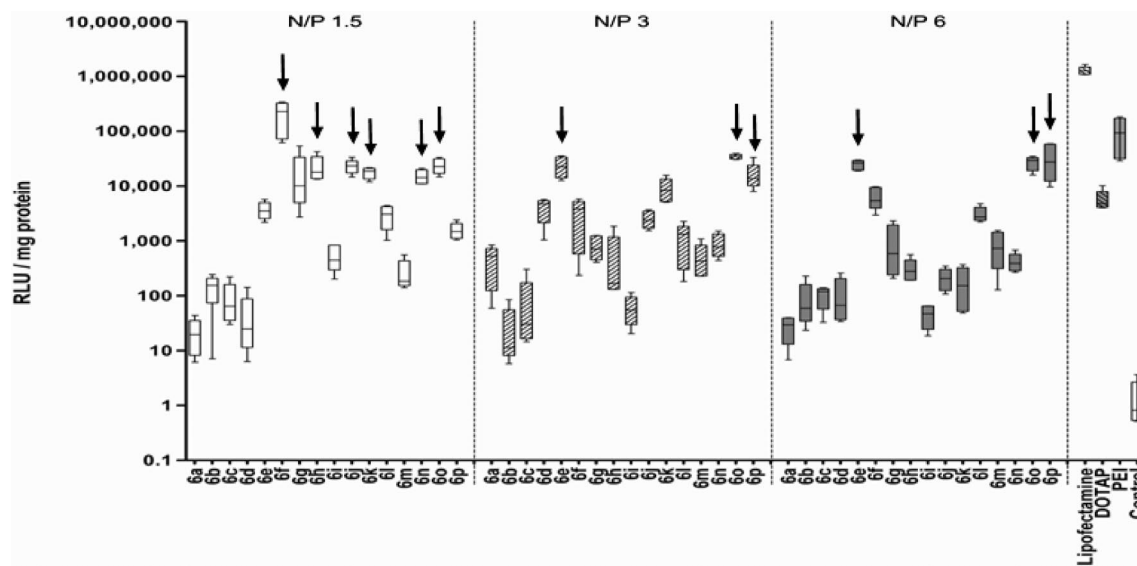


Figure 7. Luciferase activity of compounds **6a–p** complexed with pLux at various charge ratios in 16HBE14o- cells. $n = 6$ wells/group. Arrows represent $p < 0.05$ when compared to DOTAP.

1.2. Procedure for the Preparation of Intermediate 4. Tris[3-(*N*-*tert*-butoxycarbonylamino)propyl]methylamine **4** was synthesized from tris(2-cyanoethyl)nitromethane **1** as previously described.²¹

1.3. Coupling Procedure for the Preparation of Compounds 5a–p. Method A. Either the corresponding acyl chloride or cholestryl chloroformate was added dropwise into a solution of compound **4** (1 equiv), pyridine (1.1 equiv), and 4-dimethylami-

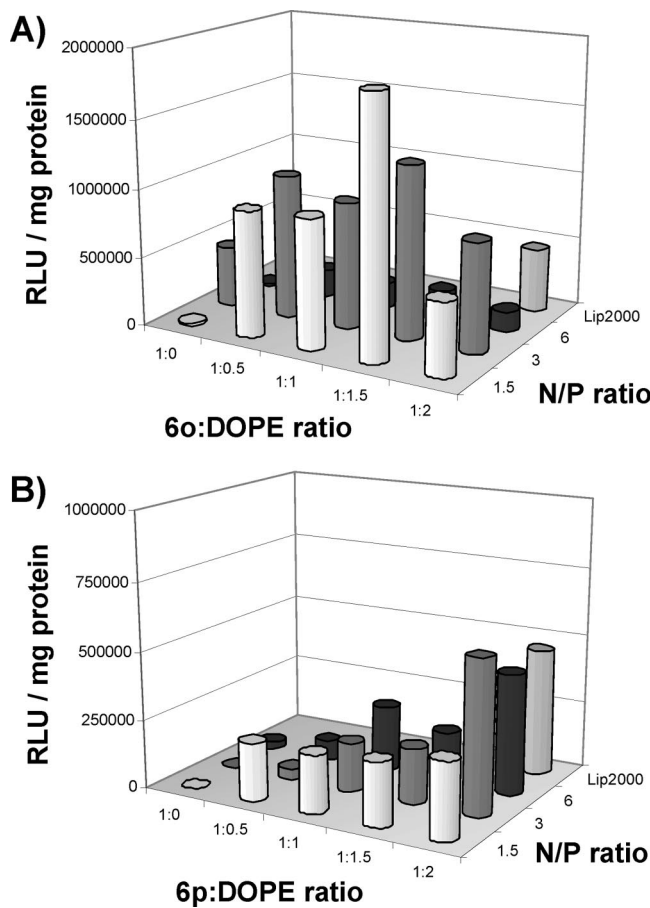


Figure 8. Luciferase activity of CHO cells after transfection with compounds **6o** (A) and **6p** (B) mixed with DOPE at a variety of molar ratios (1:0, 1:0.5, 1:1, 1:1.5, and 1:2) and complexed with pLux with charge ratios of 1.5, 3, and 6. *n* = 6 wells/group.

Table 1. Particle Size Distribution of **6o**/pLux and **6o**/DOPE/pLux Dispersions in Transfection Media

entry	N/P ratio	6o /DOPE ratio	size distribution (nm)
1	1.5	1:0	928 ± 121
2	1.5	1:0.5	1031 ± 52
3	1.5	1:1	755 ± 32
4	1.5	1:1.5	805 ± 25
5	1.5	1:2	916 ± 31
6	3	1:0	1931 ± 132
7	3	1:0.5	1019 ± 35
8	3	1:1	739 ± 26
9	3	1:1.5	652 ± 37
10	3	1:2	450 ± 45
11	6	1:0	213 ± 122
12	6	1:0.5	337 ± 66
13	6	1:1	352 ± 21
14	6	1:1.5	409 ± 38
15	6	1:2	317 ± 11

nopyridine (DMAP, 0.1 equiv) in DCM and stirred for 2 h. Subsequently the solvent was removed under vacuum, the crude was redissolved in ether, and the formed solids again were filtered off. The organic layer was then washed with water (2 × 15 mL), dried over anhydrous Na_2SO_4 , and purified by flash chromatography.

Method B. The corresponding fatty acid (1.1 equiv) and *N,N'*-dicyclohexylcarbodiimide (1.1 equiv) were dissolved in DCM and stirred for 30 min. Subsequently DMAP (0.1 equiv) and compound **4** (1 equiv) were successively added and the resulting mixture was stirred for 2 h. The solids were filtered off, and the solvent was removed under vacuum. The crude was redissolved in ether and filtered. The organic layer was then washed with water (3 × 15

mL), dried over anhydrous Na_2SO_4 , and purified by flash chromatography.

***N*-[Tris(3-(*N*-*tert*-butoxycarbonylamino)propyl)methyl]tetraecosanamide (**5o**).** Compound **5o** was synthesized following method B and purified by flash chromatography (hexanes/ethyl acetate (5:1)) to give **5o** as a white solid (91% yield): ^1H NMR (250 MHz, chloroform-*d*) δ 5.19 (br s, 1 H), 4.71 (br s, 3 H), 3.05 (br q, 6 H), 2.07 (t, *J* = 7.5 Hz, 2 H), 1.73–1.04 (m, 81 H), 0.85 (t, *J* = 6.5 Hz, 3 H); ^{13}C NMR (62.5 MHz, chloroform-*d*) δ 172.6, 156.0, 79.1, 58.0, 40.6 (CH₂), 37.5 (CH₂), 32.2 (CH₂), 31.9 (CH₂), 29.6 (CH₂), 29.5 (CH₂), 29.3 (CH₂), 28.4 (CH₃), 25.8 (CH₂), 23.8 (CH₂), 22.6 (CH₂), 14.1 (CH₃); LRMS (ES+) *m/z* 853.7 [100, (M + H)⁺].

***O*-(Cholest-5-en-3-yl)-*N*-[tris(3-(*N*-*tert*-butoxycarbonylamino)propyl)methyl]carbamate (**5p**).** Compound **5p** was synthesized following method A and purified by flash chromatography (hexanes/ethyl acetate (4:1)) to give **5p** as a white solid (83% yield): ^1H NMR (250 MHz, chloroform-*d*) δ 5.36 (br d, 1 H), 4.65 (br s, 3 H), 4.43–4.27 (m, 2 H), 3.07 (br q, 6 H), 2.40–0.74 (m, 79 H), 0.66 (s, 3 H); ^{13}C NMR (62.5 MHz, chloroform-*d*) δ 156.4, 140.1, 122.9 (CH), 79.5, 57.4 (CH₂), 57.1 (CH), 56.5 (CH), 50.4 (CH), 42.7 (CH₂), 41.1 (CH₂), 40.1 (CH₂), 39.9 (CH₂), 38.9 (CH₂), 37.4 (CH₂), 36.9 (CH₂), 36.6 (CH₂), 36.2 (CH), 32.9 (CH₂), 32.2 (CH), 28.8 (CH₃), 28.6 (CH₂), 28.5 (CH₂), 28.4 (CH), 24.6 (CH₂), 24.2 (CH₂), 23.2 (CH₃), 22.9 (CH₃), 21.4 (CH₂), 19.7 (CH₃), 19.1 (CH₃), 12.2 (CH₃); LRMS (ES+) *m/z* 915.7 [100, (M + H)⁺].

1.4. Procedure for the Preparation of Final Compounds (6a**–**p**).** Compounds **5a**–**p** (1 mmol) were dissolved in 4 N HCl in dioxane or in 2 N HCl in 1:1 water/dioxane (20 mL) and stirred for 2–4 h. The mixture was concentrated under vacuum to give rise to colorless oils, which were then dissolved in water and freeze-dried to give **6a**–**p** as white solids in quantitative yield. All compounds were slightly hygroscopic.

***N*-[Tris(3-(amino)propyl)methyl]tetraecosanamide Trihydrochloride (**6o**).** ^1H NMR (250 MHz, methanol-*d*₄) δ 7.93 (br s, 1 H), 2.94 (br t, NH_3^+), 2.23 (t, *J* = 7.0 Hz, 2 H), 1.86–1.47 (m, 14 H), 1.46–1.05 (m, 40 H), 0.90 (t, *J* = 6.5 Hz, 3 H); ^{13}C NMR (62.5 MHz, methanol-*d*₄) δ 176.5, 59.1, 41.1 (CH₂), 37.9 (CH₂), 33.1 (CH₂), 32.6 (CH₂), 30.8 (CH₂), 30.6 (CH₂), 30.5 (CH₂), 27.3 (CH₂), 23.8 (CH₂), 22.7 (CH₂), 14.5 (CH₃); LRMS (ES+) *m/z* 553.6 [100%, (M + H)⁺]; HRMS (FAB+) *m/z* calcd for $\text{C}_{34}\text{H}_{73}\text{N}_4\text{O}$ [(M + H)⁺] 553.578 44, found 553.578 31 (−0.24 ppm). Anal. ($\text{C}_{34}\text{H}_{75}\text{Cl}_3\text{N}_4\text{O}$) C, H, N.

***N*-[Tris(3-(amino)propyl)methyl]-*O*-cholesterylcaramate Trihydrochloride (**6p**).** ^1H NMR (250 MHz, methanol-*d*₄) δ 7.90 (br s, 1 H), 5.32 (br s, 1 H), 4.25 (br s, 1 H), 3.46 (q, 6 H), 2.83 (br t, NH_3^+), 2.40–0.74 (m, 79 H), 0.66 (s, 3 H); ^{13}C NMR (62.5 MHz, methanol-*d*₄) δ 156.7, 141.3, 123.4 (CH), 75.2, 66.9 (CH₂), 58.1 (CH), 57.7, 57.6 (CH), 51.7 (CH), 43.5 (CH₂), 41.1 (CH₂), 40.9 (CH₂), 40.7 (CH₂), 39.7 (CH₂), 38.3 (CH₂), 37.8 (CH₂), 37.4 (CH₂), 37.1 (CH), 33.2 (CH), 33.1 (CH₂), 32.8 (CH₂), 29.4 (CH₂), 29.3 (CH₂), 29.2 (CH), 25.4 (CH₂), 25.0 (CH₂), 23.3 (CH₃), 23.0 (CH₃), 22.5 (CH₂), 22.2 (CH₂), 19.8 (CH₃), 19.3 (CH₃), 15.5 (CH₃), 12.4 (CH₃); LRMS (ES+) *m/z* 615.5 [100%, (M + H)⁺]; HRMS (FAB+) *m/z* calcd for $\text{C}_{38}\text{H}_{71}\text{N}_4\text{O}_2$ [(M + H)⁺] 615.557 70, found 615.557 49 (−0.35 ppm). Anal. ($\text{C}_{38}\text{H}_{73}\text{Cl}_3\text{N}_4\text{O}_2 \cdot 0.6\text{H}_2\text{O}$) C, H, N.

2. Transfection Assays. 2.1. N/P Ratio (Charge Ratio). The N/P ratio is a measure of the ionic balance of the complexes. Because the main interaction between cationic lipids and nucleotides is ionic, this ratio refers to the number of protonated nitrogen residues of any transfection agent per anionic phosphate group. Since each nucleotide holds a negative charge (phosphate group), DNA normality is calculated by dividing the mass of DNA used in the experiment by the average molecular weight of a nucleotide (330 Da). Cationic lipid normality is obtained by multiplying its molarity by the number of nitrogen motifs that are expected to be protonated in neutral aqueous solution. Because the tripodal structures **6a**–**p** hold three positive charges, a charge ratio of 3 (or 3/1) means that the complex is produced by mixing one molecule of cationic lipid per equivalent of DNA (=one “unit” of the polynucleotide).

2.2. Cell Culture. Transformed African green monkey kidney fibroblast-like (Cos7) cells (LGC Promochem) were cultured in Dulbecco's modified Eagle's medium (DMEM; Invitrogen Ltd., Paisley, U.K.), supplemented with 10% fetal bovine serum (FBS; Invitrogen Ltd.), penicillin G (100 U/mL), and streptomycin sulfate (100 μ g/mL) (Invitrogen Ltd.). Transformed Chinese hamster ovary epithelial (CHO) cells (LGC Promochem) were cultured in RPMI-1640 medium (Invitrogen Ltd.), supplemented with 10% FBS, 1% L-glutamine (Invitrogen Ltd.), penicillin G (100 U/mL), and streptomycin sulfate (100 μ g/mL). Transformed human bronchial epithelial (16HBE14o-) cells were kindly supplied by Dr. D. C. Gruenert (University of California, San Francisco, CA). Cells were grown on a matrix composed of type VI mouse collagen (0.005 mg/mL; Sigma-Aldrich, Dorset, U.K.), fibronectin (0.01 mg/mL; Sigma-Aldrich), and bovine serum albumin (BSA, 0.1 mg/mL; Sigma-Aldrich) diluted in minimum essential medium (MEM; Invitrogen Ltd.) containing Earle's salts and L-glutamine. Cells were cultured in MEM containing Earle's salts and L-glutamine, 10% FBS, 1% nonessential amino acids (NEAA; Invitrogen Ltd.), penicillin G (100 U/mL), and streptomycin sulfate (100 μ g/mL).

2.3. Transfection Experiments. Cells were seeded in 96-well plates at $(1-2) \times 10^5$ cells per well and transfected when 90–100% confluent. Lipofectamine 2000 (L2000; Invitrogen Ltd.), polyethylenimine (PEI, Sigma-Aldrich), DOTAP (Roche), and tris-branched cationic lipids were complexed with a luciferase expression plasmid (pLux; kindly supplied by Dr. Deborah R Gill and Dr. Stephen C Hyde, Gene Medicine Group, University of Oxford, Oxford, U.K.) as follows: (1) pLux was complexed with L2000 at a 1:1.6 μ g/ μ L ratio according to manufacturer's instructions. (2) PEI (4.3 mg/mL diluted in water, pH7.4) was complexed, following optimized conditions within our laboratory, with pLux (1 μ g/ μ L) at a *N/P* ratio of 10:1 (pLux was slowly added to PEI with vortexing between additions). (3) DOTAP was complexed with pLux at a 6:1 (lipid/DNA) w/w ratio according to manufacturer's instructions. (4) Tris-branched cationic lipids (10 μ mol/mL in methanol) were mixed with DOPE (7 mg/mL in chloroform) at a 1:1 (lipid/DOPE) ratio and then vacuum-dried for 10 min at 60 °C. Dried lipid films were resuspended in tissue culture water and vortexed for 15 s and then sonicated for 5 min. pLux was added to the reconstituted liposomes at *N/P* ratios of 1.5:1, 3:1, and 6:1, and lipoplexes were incubated at room temperature for 15 min before being diluted in Opti-MEM. All lipoplexes were incubated with cells for 5 h (300 ng pLux/well) before the Opti-MEM was removed and replaced with medium. Opti-MEM only was added to the untransfected control group. Gene transfer was assessed 24 h after the addition of the lipoplexes.

2.4. Luciferase Reporter Gene Assay. Medium was replaced with 150 μ L of reporter lysis buffer (Promega Corporation, Southampton, U.K.), and then plates were frozen at –70 °C. After thawing on ice, cell lysates were centrifuged at 13 000 rpm for 10 min at 4 °C. Luciferase expression was measured using the Luciferase Assay System kit (Promega Corporation) according to manufacturer's instructions. Standards were prepared using recombinant firefly luciferase (QuantiLum recombinant luciferase, Promega Corporation) and BSA (Sigma-Aldrich). Luminescence was measured using a Lucy luminescence reader (Anthos, Cambridge, U.K.). Protein was measured by BCA protein assay kit (Pierce, Northumberland, U.K.) according to manufacturer's instructions.

3. Cell Viability Assay. Lipids **6a–p** (4.5, 9.1, and 18.2 μ M for *N/P* of 1.5, 3, and 6, respectively) were complexed with DOPE (same concentrations as for lipid) and pLux (300 ng/well) as described previously and added to 16HBE14o- cells. Twenty-four hours after the addition of the lipoplexes, cell death was measured using an MTT cell proliferation assay (LGC Promochem, Middlesex, U.K.), which was performed according to manufacturer's instructions. Absorbance was spectrophotometrically measured at 570 nm.

4. Particle Size Determination. Lipoplexes were formed as previously described and diluted in Opti-MEM following the

protocol used for the transfection experiments. Subsequently particle size was determined by dynamic light scattering.

5. Statistical Analysis. Groups of six experiments were analyzed using Kruskal–Wallis ANOVA and a subsequent Mann–Whitney post hoc test with a Bonferroni correction factor (*p* value multiplied by the square root of the number of groups).

Acknowledgment. We would like to thank Dr. D. C. Gruenert for supplying the 16HBE14o- cells and Dr. D. R. Gill and Dr. S. C. Hyde for supplying the luciferase expression plasmid. We thank Prof. W. Poon and Dr. A. Schofield for the particle size determination. This work has made use of the resources provided by the EaStCHEM Research Computing Facility. This facility is partially supported by the eDIKT2 initiative.

Supporting Information Available: Experimental details of the computational calculations, analysis of the RDFs, MD simulation of lipid molecule bound to DNA fragment, experimental details of compounds **5a–n** and **6a–n**, elemental analysis data of final compounds, fluorescence-based competitive assay, preliminary biological results, cytotoxicity assay, and a video file in avi format of MD trajectories of lipid. This material is available free of charge via the Internet at <http://pubs.acs.org>.

References

- (1) Baum, C.; Dullmann, J.; Li, Z.; Fehse, B.; Meyer, J.; Williams, D. A.; von Kalle, C. Side effects of retroviral gene transfer into hematopoietic stem cells. *Blood* **2003**, *101*, 2099–114.
- (2) Check, E. Gene therapists urged to learn more immunology. *Nature* **2005**, *434*, 812.
- (3) Lehn, P.; Fabrega, S.; Oudhiri, N.; Navarro, J. Gene delivery systems: bridging the gap between recombinant viruses and artificial vectors. *Adv. Drug Delivery Rev.* **1998**, *30*, 5–11.
- (4) Martin, B.; Sainlos, M.; Aissaoui, A.; Oudhiri, N.; Hauchecorne, M.; Vigneron, J.-P.; Lehn, J.-M.; Lehn, P. The design of cationic lipids for gene delivery. *Curr. Pharm. Des.* **2005**, *11*, 375–394.
- (5) Gardner, R. A.; Belting, M.; Svensson, K.; Phanstiel, O., IV. Synthesis and transfection efficiencies of new lipophilic polyamines. *J. Med. Chem.* **2007**, *50*, 308–318.
- (6) Zuhorn, I. S.; Engberts, J. B. F. N.; Hoekstra, D. Gene delivery by cationic lipid vectors: overcoming cellular barriers. *Eur. Biophys. J.* **2007**, *36*, 349–362.
- (7) Farhood, H.; Serbina, N.; Huang, L. The role of dioleoyl phosphatidylethanolamine in cationic liposome-mediated gene-transfer. *Biochim. Biophys. Acta* **1995**, *1235*, 289–295.
- (8) Ellens, H.; Bentz, J.; Szoka, F. C. Fusion of phosphatidylethanolamine-containing liposomes and mechanism of La-HII phase transition. *Biochemistry* **1986**, *25*, 4141–4147.
- (9) Koltover, I.; Salditt, T.; Raedler, J. O.; Safinya, C. R. An inverted hexagonal phase of cationic liposome–DNA complexes related to DNA release and delivery. *Science* **1998**, *281*, 78–81.
- (10) Felgner, P. L.; Gadek, T. R.; Holm, M.; Roman, R.; Chan, H. W.; Wenz, M.; Northrop, J. P.; Ringold, G. M.; Danielsen, M. Lipofection: a highly efficient, lipid-mediated DNA-transfection procedure. *Proc. Natl. Acad. Sci. U.S.A.* **1987**, *84*, 7413–7417.
- (11) Leventis, R.; Silvius, J. Interactions of mammalian cells with lipid dispersions containing novel metabolizable cationic amphiphiles. *Biochim. Biophys. Acta* **1990**, *1023*, 124–132.
- (12) Gao, X.; Huang, L. Cationic liposome-mediated gene transfer. *Gene Ther.* **1995**, *2*, 710–722.
- (13) Hofland, H. E.; Shephard, L.; Sullivan, S. M. Formation of stable cationic lipid/DNA complexes for gene transfer. *Proc. Natl. Acad. Sci. U.S.A.* **1996**, *93*, 7305–7309.
- (14) Remy, J.-S.; Sirlin, C.; Vierling, P.; Behr, J.-P. Gene transfer with a series of lipophilic DNA-binding molecules. *Bioconjugate Chem.* **1994**, *5*, 647–54.
- (15) Cantor, C. R.; Schimmel, P. R. *Biophysical Chemistry*; Freeman and Co.: San Francisco, CA, 1980.
- (16) Haldar, J.; Aswal, V. K.; Goyal, P. S.; Bhattacharya, S. Molecular modulation of surfactant aggregation in water: effect of the incorporation of multiple headgroups on micellar properties. *Angew. Chem., Int. Ed.* **2001**, *40*, 1228–1232.
- (17) Lv, H.; Zhang, S.; Wang, B.; Cui, S.; Yan, J. Toxicity of cationic lipids and cationic polymers in gene delivery. *J. Controlled Release* **2006**, *114*, 100–109.
- (18) Tang, F. X.; Hughes, J. A. Synthesis of a single-tailed cationic lipid

and investigation of its transfection. *J. Controlled Release* **1999**, *62*, 345–358.

(19) Yingyongnarongkul, B.; Howarth, M.; Elliot, T.; Bradley, M. Solid-phase synthesis of 89 polyamine-based cationic lipids for DNA delivery to mammalian cells. *Chem.—Eur. J.* **2004**, *10*, 463–473.

(20) Bloomfield, V. A. DNA condensation. *Curr. Opin. Struct. Biol.* **1996**, *6*, 334–341.

(21) Lebreton, S.; Newcombe, N.; Bradley, M. Rapid synthesis of high-loading resins using triple branched protected monomer for dendrimer synthesis. *Tetrahedron Lett.* **2002**, *43*, 2475–2478.

(22) Yan, B.; Shi, R.; Zhang, B.; Kshirsagar, T. A. Kinetic study of product cleavage reactions from the solid phase by a biocompatible and removable cleaving reagent, HCl. *J. Comb. Chem.* **2007**, *9*, 684–689.

(23) Sambrook, J.; Fritsch, E. F.; Maniatis, T. Gel Electrophoresis of DNA. In *Molecular Cloning: A Laboratory Manual*, 2nd ed.; Cold Spring Harbor Laboratory Press: New York, 1989; pp 6.3–6.34.

(24) Gill, D. R.; Smyth, S. E.; Goddard, C. A.; Pringle, I. A.; Higgins, C. F.; Colledge, W. H.; Hyde, S. C. Increased persistence of lung gene expression using plasmids containing the ubiquitin C or elongation factor 1alpha promoter. *Gene Ther.* **2001**, *8*, 1539–46.

(25) Felgner, J. H.; Kumar, R.; Sridhar, C. N.; Wheeler, C. J.; Tsai, Y. J.; Border, R.; et al. Enhanced gene delivery and mechanism studies with a novel series of cationic lipid formulations. *J. Biol. Chem.* **1994**, *269*, 2550–61.

(26) Boyd, A. C.; Porteous, D. J. Revisiting the mouse lung model for CF. *Gene Ther.* **2004**, *11*, 737–738.

(27) Hyde, S. C.; Southern, K. W.; Gileadi, U.; Fitzjohn, E. M.; Mofford, K. A.; et al. Repeat administration of DNA/liposomes to the nasal epithelium of patients with cystic fibrosis. *Gene Ther.* **2000**, *7*, 1156–1165.

(28) Porteous, D. J.; Dorin, J. R.; McLachlan, G.; Davidson-Smith, H.; Davidson, H.; et al. Evidence for safety and efficacy of DOTAP cationic liposome mediated CFTR gene transfer to the nasal epithelium of patients with cystic fibrosis. *Gene Ther.* **1997**, *4*, 210–218.

JM701493F